2010-01-01

Developments in Monitoring Techniques for Durability Assessment of Cover-zone Concrete

W.J. McCarter
Heriot-Watt University

T. M. Chrisp
Heriot-Watt University

G. Starrs
Heriot-Watt University

Niall Holmes
Dublin Institute of Technology, niall.holmes@dit.ie

L. Basheer
Queen's University - Belfast

See next page for additional authors

Recommended Citation

McCarter, W., Chrisp, T., Starrs, G., Holmes, N., Basheer, L., Basheer, M., Nanukuttan, S.: Developments in Monitoring Techniques for Durability Assessment of Cover-Zone Concrete. 2nd International Conference on Durability of Concrete Structures, Sapporo, Japan, November, 2010.

School of Civil and Building Services Engineering

Other resources

Dublin Institute of Technology *Year* 2010

DEVELOPMENTS IN MONITORING TECHNIQUES FOR DURABILITY ASSESSMENT OF COVER-ZONE CONCRETE

Niall O. Holmes
DIT, niall.holmes@dit.ie

— Use Licence —

Attribution-NonCommercial-ShareAlike 1.0

You are free:

- to copy, distribute, display, and perform the work
- to make derivative works

Under the following conditions:

- Attribution.
  You must give the original author credit.
- Non-Commercial.
  You may not use this work for commercial purposes.
- Share Alike.
  If you alter, transform, or build upon this work, you may distribute the resulting work only under a license identical to this one.

For any reuse or distribution, you must make clear to others the license terms of this work. Any of these conditions can be waived if you get permission from the author.

Your fair use and other rights are in no way affected by the above.

DEVELOPMENTS IN MONITORING TECHNIQUES FOR DURABILITY ASSESSMENT OF COVER-ZONE CONCRETE.

W. J. McCarter[(1)], T. M. Chrisp[(1)], G. Starrs[(1)]

N. Holmes[(2)], L. Basheer [(2)], M. Basheer [(2)], S. V. Nanukuttan[(2)]

(1) Heriot Watt University, School of the Built Environment, Edinburgh, Scotland, U.K.

(2) Queen's University, School of Planning, Architecture and Civil Engineering, Belfast, N. Ireland, U.K.

Abstract

This paper outlines developments in the use of an embedded multi-electrode sensor to study the response of the cover-zone (surface 50mm) to the changing ambient environment. The sensor enables the measurement of the spatial and temporal distribution of the electrical properties of concrete and temperature within the cover-zone thereby allowing an integrated assessment of cover-zone concrete performance. Both laboratory and field results are presented to highlight the information that can be obtained from embedded sensors. When exposed to the natural environment, the temperature dependence of the electrical response is highlighted and standardization protocols are developed to account for this effect. The monitoring system detailed also allows remote interrogation thereby providing (if required) a continuous output of real-time data and developments in this area are presented.

Keywords: Concrete; cover-zone; performance; monitoring; electrical properties.

1. INTRODUCTION

1.1 Background

The premature deterioration of concrete structures is a world-wide problem. In most developed countries, including the UK, around 50% of the construction budget is devoted to repair and maintenance of structures around 30% of this expenditure on concrete structures. In addition, our infrastructure has now reached an age where capital costs have decreased, but inspection and maintenance costs have grown, constituting a major part of the recurrent costs of the infrastructure. Traffic delay costs due to inspection and maintenance programmes are already estimated to be between 15%-40% of the construction costs [1]. Demands for enhanced performance create a pressing need to be able to determine, with an acceptable

degree of confidence, the anticipated service life of concrete structures. Monitoring deterioration would provide an early warning of incipient problems enabling the planning and scheduling of maintenance programmes, hence minimising traffic delays resulting from road/lane closures. The development of integrated monitoring systems for new reinforced concrete structures could also reduce costs by allowing a more rational approach to the assessment of repair options; and, co-ordination and scheduling of inspection and maintenance programmes. It is now recognised that integrated monitoring systems and procedures have an important role to play in the total management of structures. When data from monitoring systems are used with improved service-life prediction models additional savings in life cycle costs could result.

1.2 Monitoring Cover-Zone Performance

Since it is the concrete cover-zone (i.e. the covercrete) which protects the steel from the external environment, the ability to continuously monitor this zone would allow a more informed assessment of the current and future performance of reinforced concrete structures. The development of sensors and associated monitoring systems to assess covercrete performance would thus form an important element in the inspection, assessment and management of structures [2]. At present, very little in-situ monitoring of the deterioration of concrete structures is undertaken, primarily due to the lack of reliable methods that provide the information that will allow estimation of residual life. To this end, this paper highlights developments in the use a multi-electrode array embedded within the covercrete to facilitate real-time monitoring of both the spatial distribution and temporal changes in electrical conductivity (and temperature), herein after called the sensor. The electrical properties of concrete are directly related to those properties of concrete which promote the ingress of water and water containing deleterious ionic species, furthermore, once passivity has been lost, the electrical conductivity of the concrete surrounding the steel reinforcement plays an important role in corrosion dynamics [3-5].

Data are presented from specimens (laboratory and field exposure) to highlight the information that can be obtained from the sensor; also presented are preliminary results from a monitoring system currently being trialled allowing remote interrogation of specimens placed in a marine environment.

2. EXPERIMENTAL AND TEST PROCEDURES

A summary of materials, specimen fabrication, instrumentation and measurement procedures are presented below.

2.1 The Electrode Array

In summary, the sensor allows measurement of conductivity and temperature (by means of thermistors) at discrete points within the concrete cover-zone. Electrode-pairs and thermistors are mounted on a PVC former with the former being secured onto two steel bars (mild-steel/stainless-steel) as shown in Figure. 1. These bars form an integral part of the sensor as they are used to attach the array to the steel reinforcement and also form a macro-cell current measurement facility. The bars on the sensor are electrically isolated from the steel reinforcement.

Each electrode comprises a stainless steel pin (1.2mm in diameter) which is sleeved to expose a 5mm tip; in each electrode pair the pins had a (horizontal) centre to centre spacing of

5mm. The pairs of electrodes were positioned at 5, 10, 15, 20, 30, 40 and 50mm from the exposed surface. Four thermistors were also mounted on the former and positioned at 10, 20, 30 and 40mm from the exposed surface to allow measurement of the covercrete temperature. Prior to installation, the electrode arrays were calibrated in solutions of known conductivity thereby enabling the measured resistance, R (in ohms), at each electrode pair to be converted to resistivity, ρ (in ohm-m) or, its reciprocal, conductivity, σ (in Siemens/m). As the array comprises seven electrode pairs, an averaged calibration constant was evaluated for the array.

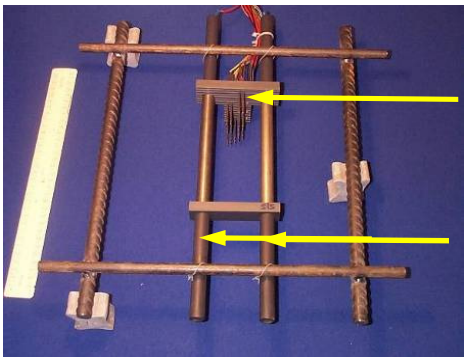

Multi-electrode and thermistor array

Rebar attachment facility forming an integral part of the unit.

Figure 1: The sensor unit.

2.2 Measurements

A battery operated data logging system was developed which comprised a central controller (for electrical measurements and data storage) connected to a multiplexing unit. The same measurement system was used for data collection for both laboratory and site-based specimens. Electrical measurements from the sensor are obtained using a battery operated, auto-ranging resistance logger which measured the resistance using an a.c. excitation voltage of 1.0V at a frequency of 1kHz. Preliminary studies indicated that the chosen operating voltage amplitude and frequency would ensure electrode polarisation effects were minimised. The logger was designed to record resistance data into a non-volatile memory which were periodically downloaded to a computer. Data were then converted to concrete resistivity; thermistor measurements were also logged using the same system with resistance measurements converted to temperature using the Steinhart-Hart equation with appropriate conversion factors.

2.3 Materials, Samples and Curing

Mixes were chosen to satisfy the requirements for virtually all exposure conditions specified in EN 206-1:2000 [6]. Dredged river gravel and matching fine aggregate were used; the binders comprised ordinary Portland cement (OPC) CEM I 42.5N (EN197-1:2000 [7]); CEM I cement blended with ground granulated blast-furnace slag (GGBS) (EN15167-1:2006 [8]); and CEM I cement blended with fly-ash (EN 450-1:2005 [9]) (see Table 1). Specimens were 300×300×150mm (thick) slabs, with the working face cast against plywood formwork. The plywood formwork had been given a coat of proprietary release agent prior to casting. The multi-electrode array, described above, was placed at the plan centre of each slab. On demoulding, the samples were wrapped with damp hessian and polythene for a period of 7 days. All surfaces, apart from the surface cast against the formwork that was to be used as the exposed working surface, were then sealed with several coats of an epoxy-based paint to ensure 1-dimensional drying/absorption. Thereafter, samples were left in a laboratory (20°C±1°C; 50-55%RH) until required for testing.

(i) Laboratory Exposure: after 6 weeks air-curing under laboratory conditions, water was supplied from a reservoir placed over the full suction surface (300×300mm^2) of the sample (i.e. the bottom surface of the slab cast against formwork) and maintained for a period of 48-hours. The samples were then subjected to a cyclic regime of approximately 8 weeks drying followed by a further 48-hour water absorption.

(ii) Marine Exposure: a total of 54 samples (18 of each mix) were placed at a marine exposure site on the Dornoch Firth (Scotland) and positioned at three environmental exposures: above high-water-level (airborne spray zone: XS1[6]); just below high-water-level (tidal/splash zone: XS3 [6]), and below mid-tide level (submerged zone: XS2 [6]). This is discussed below. The concrete blocks were saturated with water to prevent excessive absorption of seawater on placement.

Table 1. Summary of concrete mixes.

MIX	CEM I 42.5N	CEM III/A	CEM II/B-V
OPC	460	270	370
GGBS	-	180	-
Fly Ash		-	160
(kg/m^3)			
20mm	700	700	695
10mm	350	375	345
fine	700	745	635
(kg/m^3)			
Plasticiser (l/m^3)	1.84	3.60	2.65
w/b*	0.4	0.44	0.39
Slump (mm)	105	140	110
F_{28} (MPa)	70	53	58

* water/binder ratio where binder comprises OPC + replacement.

3. RESULTS AND DISCUSSION

At a frequency of 1kHz, the electrical resistance of concrete will be dominated by electrolytic conduction through the water-filled capillary pores and will thus be dependent upon:

(a) hydration and pozzolanic reaction (and, when chlorides are present, chloride binding effects). This has the effect of increasing pore constriction and tortuosity thereby increasing the resistivity over the longer term;
(b) surface drying effects which will increase resitivity; and,
(c) water ingress, which will result in an decrease in the measured resistivity (enhanced by chlorides, if present within the invading solution).

Data are presented to illustrate the above effects and highlight the information which can be obtained from the sensor.

3.1 Absorption

Conditioned slabs were ponded with water and resistance measurements monitored on a ten minute cycle over a 48-hour period. Figure 2 presents typical responses from the electrode-pairs placed at the respective depths and noted beside each curve. In this Figure, the change in resistance relative to its value prior to absorption is presented and denoted R_r; R_r is defined as the ratio R_t/R_o where R_o is the resistance measured across a particular electrode pair just before the start of the absorption test and R_t is the resistance measured across the respective pair at time, t, after the start of the absorption test. As the water-front moves into the cover-zone it would be anticipated that R_r will decrease relative to its initial value of 1.0. With reference to Figure 3, the response at any depth comprises one or more of the following regions:

(I) An initial region where R_r remains relatively constant although, in some instances, an increase is detected. Regarding the latter, we attribute this to the air in the partially saturated capillary pores being pushed ahead of the advancing water-front and dispersing into the pore system;

(II) A decreasing portion of the curve where the advancing water-front moves into the vicinity of the electrical field between the electrodes and eventually beyond its zone of influence; and,

(III) A further region where R_r attains a steady-state value. When a steady state R_r value has been achieved at a particular depth, the water front has advanced beyond that particular electrode level. The void network could be considered fully saturated in the vicinity of that electrode level.

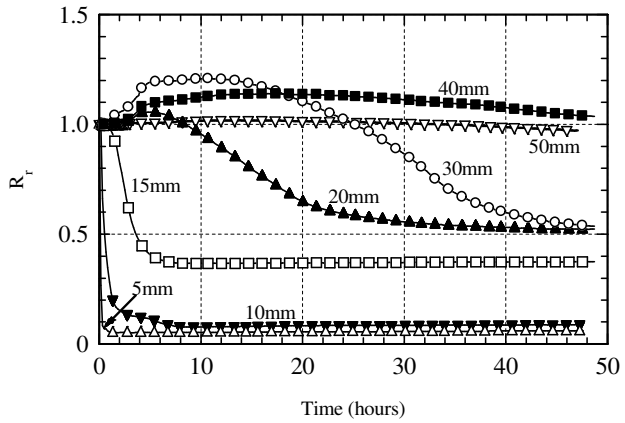

Figure 2: Variation in R_r during absorption.

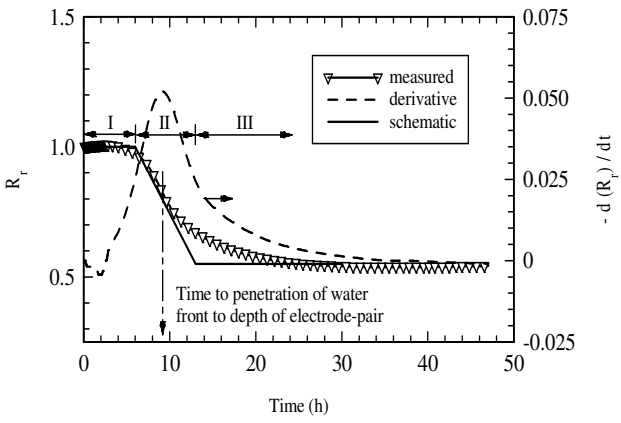

Figure 3: Schematic for R_r during absorption and derivative to estimate time of arrival of water-front.

It is evident from Figure 2 that where a steady-state value of R_r has been achieved, this value increases with increasing depth from the surface. The steady-state value of R_r (denoted $R_{r,ss}$) can be related to the initial degree of saturation, S_r, of the void system in the vicinity of the electrodes i.e. the degree of capillary pore saturation **prior** to absorption. The following relationship, which has been used on rock formations [10], could be applied,

$$S_r \approx \sqrt[m]{\frac{R_{sat}}{R_o}} = \sqrt[m]{R_{r,ss}} \quad (1)$$

where R_{sat} is the resistance of the fully saturated concrete; R_o is the resistance of the concrete at degree of saturation S_r, and *m* is a cementation factor. Values of *m* for rocks [10] lie in the region 2-3. Little work has been published on *m* values for concretes, however, values for ordinary Portland cement pastes [11] have been quoted in the range 1.5-3.5. This could allow an estimation of the saturation gradient through the cover-zone after the period of drying.

3.2 Cyclic Wetting and Drying

Since drying involves vapour transfer to the exposed concrete surface, this results in the development of a *saturation* or *moisture gradient* through the cover-zone. Since the degree of saturation of the concrete has a significant influence on the capillary suction forces the drying response of the cover-zone is another characteristic which influences its performance. The response of the cover to a controlled cyclic wetting/drying regime is presented in Figure 4 for CEM I (Figure 4(a)) and CEM II/B-V (Figure 4(b)) mixes. As anticipated, the resistivity, ρ_t, increases during drying and decreases under wetting, although it is evident that this effect diminishes with increasing depth through the cover. Regarding the latter, only those electrodes positioned within the surface 30mm or so, indicate that the period of drying has influenced this region of the cover-zone. It is also apparent that the resistivity at a depth of 50mm displays a continual increase with time, and is particularly evident for the fly-ash concrete (Figure 4(b)). This is attributed to on-going hydration and pozzolanic reaction during the post curing period and indicates 'self-curing' processes - it also results in considerably higher resistivity values for the concrete mix containing fly-ash replacement (although not presented in Figure 4, a similar feature was evident for the mix with GGBS replacement).

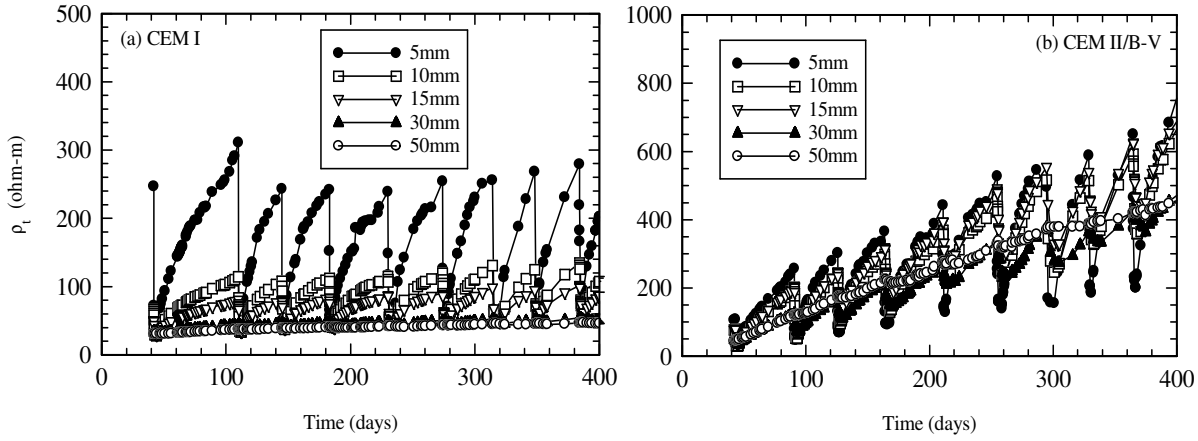

Figure 4: Cover-zone response to cycles of drying and wetting for (a) CEMI mix and (b) CEMII/B-V mix.

3.3 The Convective Zone

Figures 5(a) and (b) present, respectively, the resistivity versus depth profiles for the CEM I and CEM II/B-V concrete specimens taken at the end of a drying cycle and immediately

after 48-hours ponding with water. For illustrative purposes, this is presented for the $8^{th}/9^{th}$ drying/wetting cycles. The resistivity profile after drying decreases with distance from the exposed surface and reflects the increasing degree of pore saturation with depth; after absorption, however, the resistivity reduces markedly, particularly within the surface 30mm. Considering the profiles before and after absorption, there is a point within the cover-zone where the profiles remain virtually unchanged; this point is taken as an estimate of the depth of the cover-zone most influenced by drying action prior to absorption i.e. the *convective zone* [12].

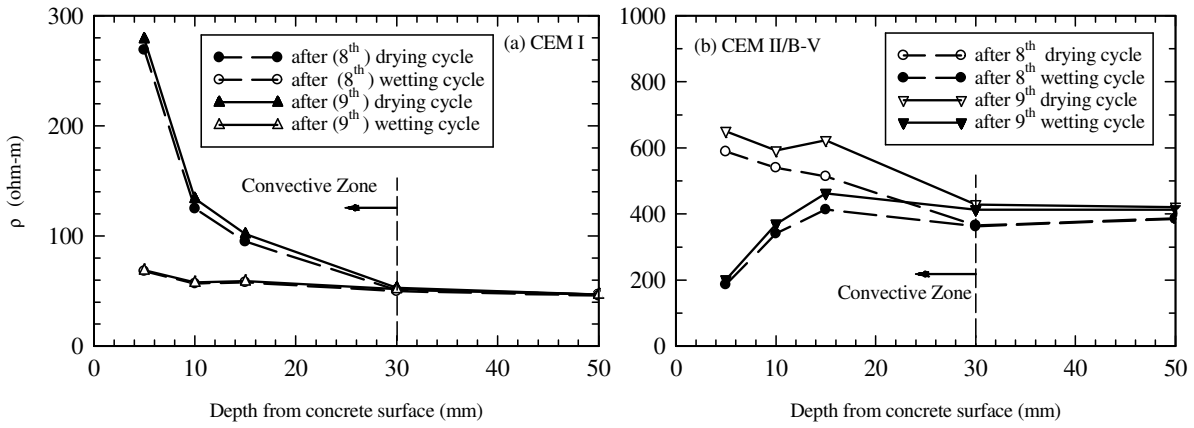

Figure 5: Resistivity profiles after drying / wetting for (a) CEMI mix; and, (b) CEMII/B-V mix.

3.4 Field Studies

Since electrical conduction through saturated concrete will be dominated by electrolytic effects, it will, as a consequence, be temperature dependent. For concrete exposed to the natural environment the seasonal change in temperature can vary markedly. As noted above, samples were deployed at a marine exposure site on the Dornoch Firth (Scotland) and the embedded sensor system interrogated remotely. The system is accessed via the mobile telephone network and powered by a battery which is charged via a solar panel. The time interval between measurement cycles is set remotely and, in this is current trial, is 12 hours. During a measurement cycle, cover-zone resistance and thermistor data are recorded for all sensor units which are subsequently stored; the systems then *sleeps* until the next measurement sequence is triggered. The data can be accessed and downloaded at any time.

For illustrative purposes, initial data are presented in Figure 6 for the CEM III/A concrete mix: XS2 environment (i.e. below mid-tide level). For clarity, only the response for electrodes positioned at 10mm and 30mm are presented together with the temperature at these locations over the same period. From Figures 6(a) and (b), it is evident that the resistivity fluctuates in sympathy with the changing temperature. In attempting to interpret these measurements, it is important to distinguish between changes in resistivity due to temperature effects and changes in resistivity due ionic ingress, changing levels of moisture content or hydration effects. In the current work, an Arrhenius relationship is used to model the influence of temperature on resistivity [13] through the equation,

$$\rho = Ae^{\left[\frac{E_a}{R_g T}\right]} \quad (2)$$

where ρ is resistivity (ohm-m) at temperature T (K); A is the nominal resistivity at infinite temperature (ohm-m); E_a is activation energy for conduction (kJ/mole); and R_g is the gas constant, 8.3141J/mole/K. Now, if ρ_x and ρ_y is the resistivity at temperatures T_x and T_y, respectively, then, from equation (2) above,

$$\rho_x = \rho_y e^{\frac{E_a}{R_g}\left[\frac{1}{T_x} - \frac{1}{T_y}\right]} \quad (3)$$

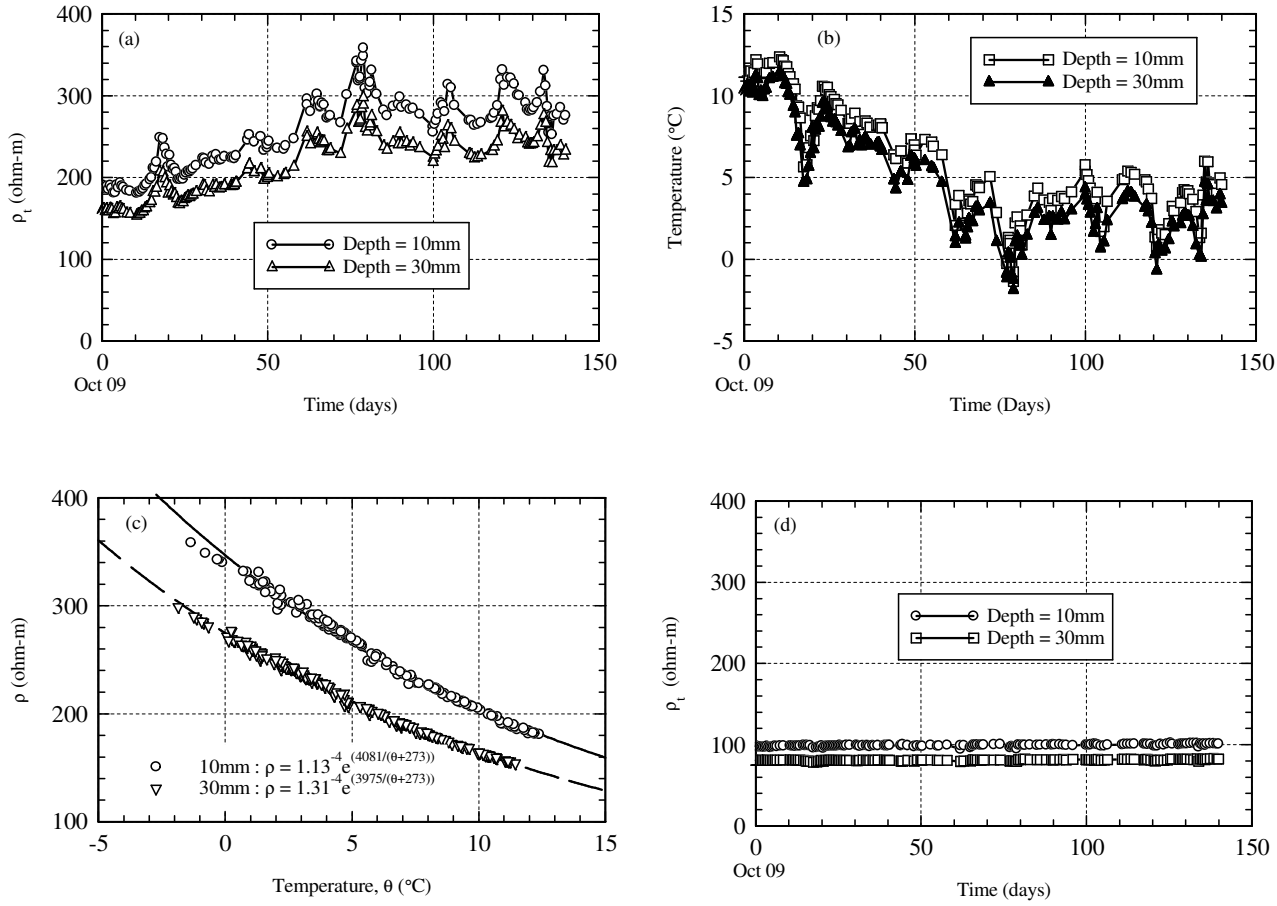

Figure 6: (a) The *as-measured* resistivity for CEM III/A concrete; (b) temperature variation within the cover-zone; (c) Arrhenius plot for data in (a) and (b); and, (d) measurements in (a) standardised to a reference temperature of 25°C.

Equation (3) implies that a value of resistivity, ρ_y, recorded at a temperature T_y could be corrected for temperature by *standardizing* the as-measured resistivity to an equivalent resistivity, ρ_x, at a reference temperature, T_x, through a knowledge of the activation energy, E_a, for the conduction process. Figure 6(c) displays the data in Figure 6(a) and (b) in the

format of equation (2) which enables evaluation of the activation energy, E_a, at the respective electrode depth. For comparison, Table 2 presents the values of E_a for all three mixes at a depth of 10mm and 30mm. It is interesting to note that the activation energy increases in the order OPC, Fly-ash, GGBS; this parameter must be related to the pore size distribution, pore connectivity and pore tortuosity, the detailed discussion of which is outwith the scope of this paper.

Table 2. Activation energy, E_a (kJ/mole), for all concrete mixes obtained from field data.

Depth	CEM I	CEM III/A	CEM II/B-V
10 mm	27.03	33.93	31.09
30 mm	27.89	33.05	30.27

Having obtained the activation energy for each electrode pair on the array, the resistivity values can now be standardised to a reference temperature through equation (3) above. Figure 6(d) displays the field measurements in Figure 6(a) standardized to a reference of 25°C. It is immediately apparent that once temperature effects have been removed from the resistivity, only minor fluctuations are evident. Using in-situ measurements allows *fine-tuning* of the activation energy for the particular concrete mix/sensor, which is more appropriate than using a *blanket* value for all concretes determined from laboratory tests. Furthermore, the activation energy is constantly updated as temperature and concrete resistivity measurements become available and provide *feed-back* into the Arrhenius equation.

The as-measured resistivity values are also of importance as, once depassified, corrosion rate is a function of the resistivity of the concrete between the anodic and cathodic areas on the rebar. There is a considerable body of published work to indicate a direct relationship between corrosion rate and concrete resistivity for depassified concrete [14-16]. Hence, as the temperature of the concrete decreases, it becomes more resistive and, as a consequence, the corrosion rate will be reduced.

4. CONCLUDING COMMENTS

It has been shown that discretized resistivity measurements allow an integrated assessment of the cover-zone and provide detailed information on both the spatial and temporal response of the cover-zone to the external environment. When exposed to the natural environment, it was shown that the electrical resistivity fluctuates in sympathy with the temperature and protocols were developed to standardize resistivity measurements to a reference temperature thereby allowing this effect to be removed from the data. Regular monitoring is important as this will, ultimately, enable evaluation of the response of the cover-zone to different ambient environments, evaluation of seasonal changes etc. As shown, the methodology lends itself to remote integration thereby allowing virtually continuous, real-time monitoring of the performance of the cover-zone and work is continuing in this respect. Instrumentation of structures with appropriate sensors such as the one described could, ultimately, play an important role in maintenance strategies and service life prediction.

ACKNOWLEDGEMENTS

The Authors acknowledge the financial support of Transport Scotland (Scottish Government) and the Engineering and Physical Sciences Research Council, U.K. (Grant EP/G025096/1). The views expressed in this paper are those of the Authors and not necessarily those of Transport Scotland.

REFERENCES

[1] 'Smart Structures: integrated monitoring systems for durability assessment of concrete structures', FORCE Institute (Denmark) Newsletter, No. 1, April, 2000, 1-2.

[2] Buenfeld, N. R., Davies, R., Karimi, A and Gilbertson, A., 'Intelligent Monitoring of Concrete Structures', CIRIA Report (C661), Jan. 2008, ISBN 978-0-86017-661-9.

[3] Broomfield, J. P., 'Corrosion of steel in concrete', E&FN Spon, London, 1997, 240pp, (ISBN 0 419 19630 7).

[4] European Union – Brite EuRam III, 'Duracrete – Modelling of degradation', Report BE95-1347/R4-5, 1998, Dec., 174pp, (ISBN 90 376 0444 7).

[5] European Union – Brite EuRam III, 'Duracrete – Models for environmental actions on concrete structures' Report BE95-1347/R3, 1999, Mar., 273pp, (ISBN 90 376 0400 5).

[6] European Committee for Standardization (CEN), EN 206-1: 2000, 'Concrete – Part 1: Specification, Performance, Production and Conformity', Brussels.

[7] European Committee for Standardization (CEN), EN 197-1: 2000, 'Cement – Part 1: Composition, specifications and conformity criteria for common cements', Brussels.

[8] European Committee for Standardization (CEN), EN 15167-1:2006, 'Ground granulated blast furnace slag for use in concrete, mortar and grout. Definitions, specifications and conformity criteria', Brussels

[9] European Committee for Standardization (CEN), EN 450-1:2005, ' Fly ash for concrete. Part 1. Definition, specifications and conformity criteria', Brussels

[10] Dullien F. A. L., 'Porous media: fluid transport and pore structure', Academic Press Inc., London, 2nd Edition, 1992.

[11] Christensen B. J. et al, 'Impedance spectroscopy of hydrating cement-based materials: measurement, interpretation, and applications', J. of the Amer. Ceram. Soc., Vol. 77, No. 11, 1994, pp2789-2804.

[12] Tuutti, K., 'Effect of cement type and different additions on service life', Proc. of the Concrete 2000 Conf., Vol. 2, E&FN Spon (Edited by R. K. Dhir and M. R. Jones), London, U.K., Vol. 2, 1993, pp.1285-1295.

[13] Chrisp, T. M., Starrs, G., McCarter, W. J., Rouchotas, E. and Blewett, J., 'Temperature-conductivity relationships for concrete: an activation energy approach', J. Matl. Science Letters, 20, 12, 2001, 1085-1087.

[14] Alonso, C., Andrade, C. and Gonzalez, J. A., 'Relation between resistivity and corrosion rate of reinforcements in carbonated mortar made with several cement types', Cem. Concr. Res., 8 (5) (1988) 687-698.

[15] Broomfield, J. P., 'Corrosion of steel in concrete', E&FN Spon, London, 1997, 240pp, (ISBN 0 419 19630 7).

[16] Gowers, K. R. and Millard, S. G., 'Measurement of concrete resistivity for assessment of corrosion severity of steel using Wenner technique', ACI Materials J., 96 (5) (1999) 536-541.